Neural Networks 22 (2009) 1334–1339

Contents lists available at ScienceDirect

Neural Networks

journal homepage: www.elsevier.com/locate/neunet

2009 Special Issue

Single-trial classification of vowel speech imagery using common spatial patterns

Charles S. DaSalla [a,c,*], Hiroyuki Kambara [b,c], Makoto Sato [b], Yasuharu Koike [b,c]

[a] Department of Computational Intelligence and Systems Science, Tokyo Institute of Technology, Yokohama, Japan

[b] Precision and Intelligence Laboratory, Tokyo Institute of Technology, Yokohama, Japan

[c] Core Research for Evolution Science and Technology (CREST), Japan Science and Technology Agency, Kawaguchi, Japan

ARTICLE INFO

Article history:
Received 7 October 2008
Received in revised form 7 May 2009
Accepted 20 May 2009

Keywords:
EEG
Vowel
Speech
Imagery
CSP

ABSTRACT

With the goal of providing a speech prosthesis for individuals with severe communication impairments, we propose a control scheme for brain–computer interfaces using vowel speech imagery. Electroencephalography was recorded in three healthy subjects for three tasks, imaginary speech of the English vowels /a/ and /u/, and a no action state as control. Trial averages revealed readiness potentials at 200 ms after stimulus and speech related potentials peaking after 350 ms. Spatial filters optimized for task discrimination were designed using the common spatial patterns method, and the resultant feature vectors were classified using a nonlinear support vector machine. Overall classification accuracies ranged from 68% to 78%. Results indicate significant potential for the use of vowel speech imagery as a speech prosthesis controller.

1. Introduction

Typical forms of communication between humans involve the conveyance of verbal or visual information, most often through vocal speech or physical gestures. Yet for severely handicapped individuals, such as those with advanced amyotrophic lateral sclerosis (ALS) or locked-in syndrome, their conditions prohibit normal communication, adversely affecting their quality of life. In recent studies, brain–computer interfaces (BCI) have been developed to provide a means of communication for such individuals who have lost the ability to communicate. Naito et al. (2007) developed a 'yes' or 'no' communication system for ALS locked-in patients by measuring hemodynamic responses in the brain using near-infrared spectroscopy. However, due to the slow nature of the hemodynamic response, over 30 s (including rest intervals) were required for one measurement sequence. Also, the control scheme applied in their system has no correlation with normal communication methods, using tasks like mental calculation, number counting, etc.

A neural response to oddball stimuli called the P300 potential has also been widely studied as a BCI controller. Nijboer et al. (2008) exploited P300 potentials in ALS patients watching a flashing matrix of letters, allowing them to spell out statements. However, since the P300 potential is not a volitive response (i.e. requires an external stimulus), it also has little correlation with normal communication.

The goal of our study is to develop the framework for a communication BCI which employs a more natural control scheme, utilizing the neural activities associated with speech production. It has been demonstrated that neural activations occur in the motor cortex during imaginary movements of the limbs and can be harnessed to control prostheses (Pfurtscheller & Neuper, 2001). It has also been demonstrated that motor cortex activations occur during the mental rehearsal of vowels (Callan, Callan, Honda, & Masaki, 2000; Fujimaki, Takeuchi, Kobayashi, Kuriki, & Hasuo, 1994). We endeavor to exploit these speech related potentials (SRP) to control a speech prosthesis (Fig. 1).

In our study, we recorded electroencephalograms (EEG) in three healthy subjects during the performance of three mental tasks, imaginary speech of the English vowels /a/ and /u/, and a no action state as control. Continuous EEG recordings were bandpass filtered and divided into epochs. SRPs were visualized through trial averaging. Using the common spatial patterns (CSP) method, we designed spatial filters which, when applied to the EEG time series, produced new time series optimized for discrimination (Ramoser, Müller-Gerking, & Pfurtscheller, 2000). We used a nonlinear support vector machine (SVM) to classify the feature vectors into the three tasks. With overall accuracies reaching up to 78%, our system proves to have significant potential as a control scheme for communication BCIs.

2. Methods

2.1. Subjects

Three subjects, 2 male and 1 female, 26–29 years of age, participated in the study. All subjects were right-handed, as

* Corresponding address: Department of Computational Intelligence and Systems Science, Tokyo Institute of Technology, 4259 Nagatsuta R2-15, Midori-ku, Yokohama, 226-8503, Japan. Tel.: +81 45 924 5086; fax: +81 45 924 5016.
E-mail address: dasalla@hi.pi.titech.ac.jp (C.S. DaSalla).

0893-6080/$ – see front matter © 2009 Elsevier Ltd. All rights reserved.
doi:10.1016/j.neunet.2009.05.008

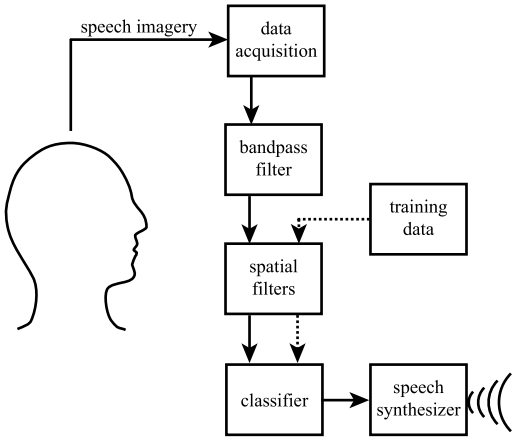

Fig. 1. Scheme for a speech prosthesis using speech imagery.

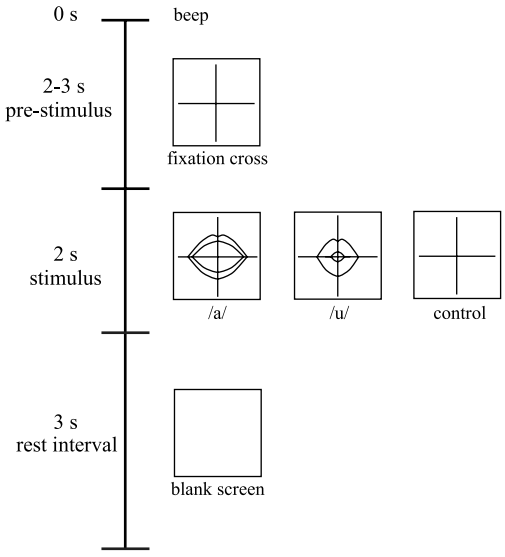

Fig. 2. Timing for one experimental trial.

assessed by the Edinburgh Inventory (Oldfield, 1971), and fluent in English. None of the participants had any known neurological disorders or other significant health problems. The experiment was conducted in accordance with the Declaration of Helsinki, and informed consent was obtained from all subjects.

2.2. Experimental paradigm

The subjects were comfortably seated in a reclining armchair. Subjects were instructed to perform one of three tasks on appearance of a visual cue:

1. Vowel /a/ — imagined mouth opening and imagined vocalization
2. Vowel /u/ — imagined lip rounding and imagined vocalization
3. Control — alert, no action

The vowels /a/ and /u/ were specifically chosen due to their dissimilar muscle activations during real speech production. Vowel /a/ is produced with mouth opening controlled by the digastricus, while /u/ is produced with lip rounding controlled by the orbicularis oris (Gray, 2000).

The subjects were coached beforehand and rehearsed with real movements to ensure correct task execution. The timing for experimental trials (Fig. 2) was organized in the following manner. Visual cues were displayed on a computer monitor placed in front of the subject, approximately 1 m away. Each trial began with an audible beep and appearance of a fixation cross. The fixation cross remained on the screen for a randomized time interval between 2 to 3 s. This gave the subject time to fixate on the cross and allowed any auditory evoked potentials caused by the beep to pass before task onset. The time interval was randomized to prevent subjects from predicting the instance of task onset. After this, a randomly selected visual cue appeared, prompting the subject to perform one of the three tasks. Vowel /a/ was represented with an image of an open mouth, vowel /u/ with an image of rounded lips, and control with a continuation of the fixation cross. The visual cue remained on the screen for 2 s. Subjects were instructed to perform and maintain the appropriate task until the visual cue disappeared 2 s later. To clarify, in task /u/, for example, subjects imagined static rounded lips and /u/ vocalization continuously for 2 s. After the visual cue disappeared, a 3 s rest interval, represented with a blank white screen, was provided before the start of the next trial. 50 trials were performed for each task, resulting in a total of 150 trials per subject.

2.3. Recording

Continuous EEG was recorded using a BioSemi ActiveTwo system (BioSemi B.V., Amsterdam, Netherlands) with 64 + 8 active Ag–AgCl electrodes and a sampling rate of 2048 Hz. To reduce file size, data was downsampled in software to 256 Hz. A BioSemi headcap (BioSemi B.V.) was used to position the 64 EEG electrodes on the scalp, according to the international 10-20 system. For EEG reference, 1 EX electrode was placed on the right mastoid. 2 EX electrodes were used to measure vertical and horizontal electrooculography. 2 EX electrodes were used to detect unwanted mouth electromyography (EMG), one placed below the jaw to detect activations of the digastricus and the other immediately lateral to the right lip crease for the orbicularis oris. The remaining 3 EX electrodes were unused. Signals were visually inspected during the recordings. Trials showing movement artifact were marked for rejection and repeated in an extra session. Only 4 trials in one subject (S2) needed to be rejected and repeated in this fashion.

2.4. Data processing

All data processing was performed offline using MATLAB R2006 (The MathWorks, Inc., Natick, MA) and EEGLAB (Delorme & Makeig, 2004). Recorded EEG data was zero-phase bandpass filtered at a range of 1–45 Hz to remove any low frequency baseline shifts and electronic noise. Epochs were extracted in reference to the stimulus onset. Each epoch had a duration of 3 s, 1 s of pre-stimulus and 2 s of stimulus. 50 epochs were extracted for each task, for a total of 150 epochs per subject.

2.5. Common spatial patterns

Using the CSP method, we designed spatial filters which, when applied to the EEG data, produce new time series with variances that are maximally discriminative. In-depth descriptions of the CSP method with equivalent equations can be found in Müller-Gerking, Pfurtscheller, and Flyvbjerg (1999) and Ramoser et al. (2000). To describe briefly, given two groups of EEG time series data (e.g. tasks /a/ and /u/), we denote each epoch as a matrix E_g^i, where the rows and columns of E are channels and samples respectively, i is the epoch label and g is the group label. We then compute normalized covariance matrices C_g for the epochs of each group and average them such that

$$\bar{C_g} = \frac{1}{n}\sum_{i=1}^{n}\frac{E_g^i(E_g^i)^{\mathrm{T}}}{trace(E_g^i(E_g^i)^{\mathrm{T}})}, \quad (1)$$

where n is the number of trials in group g. The two resultant matrices are summed to produce a composite covariance matrix C_c, which is then factored into its eigenvectors such that

$$C_c = \bar{C}_1 + \bar{C}_2 \tag{2}$$

$$C_c = V_c \lambda_c V_c^{\mathrm{T}}, \tag{3}$$

where V_c is a matrix of eigenvectors and λ_c is a diagonal matrix of eigenvalues. We then calculate a linear transformation called a "whitening transformation"

$$W = \sqrt{\lambda_c^{-1}} V_c^{\mathrm{T}} \tag{4}$$

which equalizes the variances in eigenspace. The whitening transformation is then applied to the original two covariance matrices,

$$S_g = W \bar{C}_g W^{\mathrm{T}} \tag{5}$$

$$S_1 = U \lambda_1 U^{\mathrm{T}} \quad \text{and} \quad S_2 = U \lambda_2 U^{\mathrm{T}}, \tag{6}$$

rendering their eigenvectors U equivalent and their eigenvalues λ_1 and λ_2 summing to 1, with the diagonal elements of λ_1 ordered in ascending order. Lastly, we define a projection matrix $P = (U^{\mathrm{T}} W)^{\mathrm{T}}$, where the columns of P^{-1} are the common spatial patterns and can be seen as time-invariant EEG source distribution vectors, and then decompose each EEG epoch such that

$$Z_g^i = P E_g^i. \tag{7}$$

The resultant feature vectors of Z_g^i are optimized for discriminating the two groups. Additionally, Müller-Gerking et al. (1999) showed that only the first and last two filters are needed for classification, as using more does not improve accuracy significantly.

2.6. Support vector machine

For our system, we required a classifier that has strong generalization performance, an acceptable training time, can solve multi-class problems in future designs, and is logistically simple to implement. For these reasons, we selected an SVM.

SVMs operate by identifying the optimal separating hyperplane between bordering input vectors of different classes, i.e. support vectors (Gunn, 1998). In the case of nonlinear SVMs, data is implicitly mapped into higher dimensions using a kernel function. The process is referred to as "implicit mapping" because only dot products are calculated, not the specific vector elements in higher dimensional space (DaSalla, Sato, & Koike, 2007). Although SVMs support both linear and nonlinear classification, we found that using a nonlinear classifier provided the best accuracies for our data.

Using LIBSVM, an SVM software package by Chang and Lin (2008), we applied a two-class nonlinear SVM to classify feature vectors into one of the three tasks. A radial basis function was used for the SVM kernel

$$K(x, x') = \mathrm{e}^{-\gamma \|x - x'\|^2}, \tag{8}$$

where K is a kernel function of support vectors x and pattern vectors x', and γ is a parameter determined through a grid search and cross validation of the training data (Hsu, Chang, & Lin, 2003). More specifically, a range of γ values are each tested in a v-fold cross validation of the training data. The value which provides the highest accuracy is selected for the classifier.

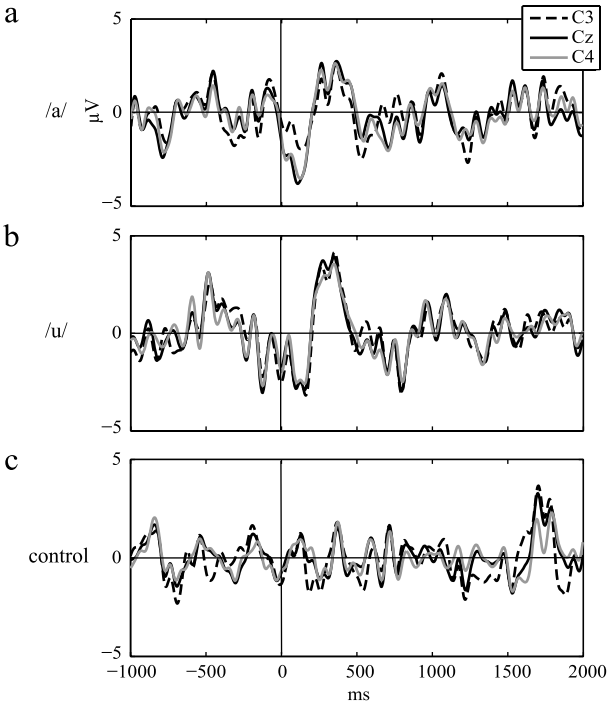

Fig. 3. Grand averages of all epochs for each task at electrode positions C3, Cz, and C4. (a) task /a/, (b) task /u/, (c) control task. Time 0 ms marks the start of the visual cue. SRPs for tasks /a/ and /u/ are visible from approximately 0 to 500 ms.

2.7. Classification

To perform the classification, we first combined all the EEG epochs of two tasks for one subject. Since CSP can only distinguish between two states, the algorithm was restricted to pairwise classifications. For all epochs, we selected a time window from 0 to 500 ms (starting at the appearance of the visual cue). We then divided the EEG data into training and testing subsets. The training set consisted of 30 of the 50 epochs per task, selected randomly. We designed spatial filters by applying the CSP method on the 30 epoch training sets, as described in Section 2.5. EEG training and testing data was decomposed using the spatial filters. The resultant spatially filtered time series were used, with no further processing, as feature vectors for classification. We trained an SVM using the feature vectors of the training set, and then evaluated it using the testing set. We repeated this procedure 20 times on randomly produced subsets for all three pairwise combinations and for each subject, thereby achieving a 20X cross validation.

3. Results

3.1. Speech related potentials

To visualize the SRPs in time series, we calculated the average of all epochs for each task across all subjects. A zero-phase finite impulse response lowpass filter with a 15 Hz cutoff was applied to the average waveforms to improve visibility. Fig. 3(a)–(c) shows grand averages for each task at electrode positions C3, Cz, and C4 of the international 10-20 system. The time 0 ms coincides with the appearance of the task specific visual cue.

For speech imagery tasks /a/ and /u/ (Fig. 3(a) and Fig. 3(b), respectively), SRPs are found following the start of the visual cue, recognized by the negative trend after time 0 ms followed by a strong positive shift at approximately 300 ms. These waveforms closely resemble movement related potentials associated with real speech movements (Deecke, Engel, Lang, & Kornhuber, 1986;

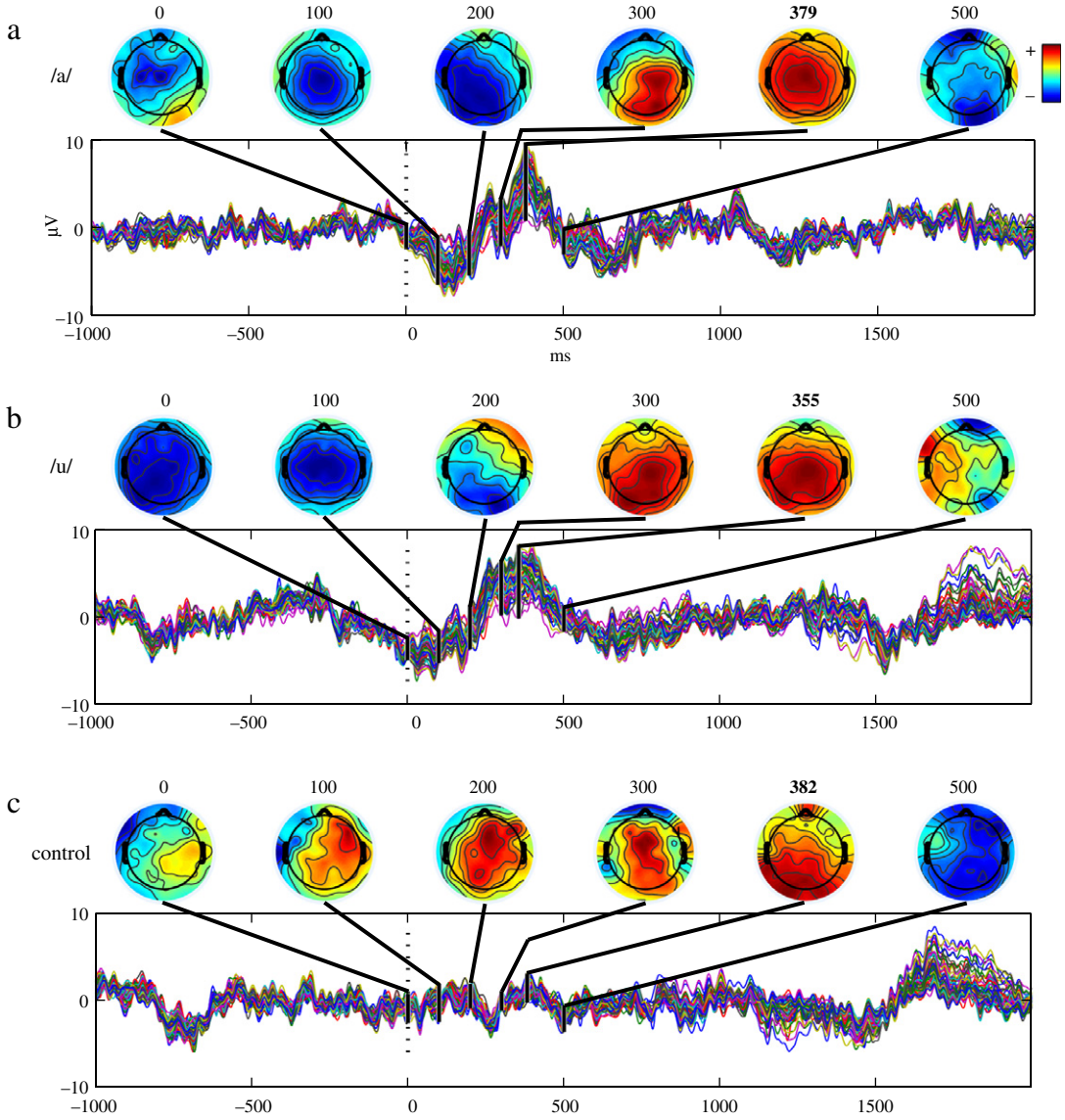

Fig. 4. Averages over 50 epochs/task for S1, with scalp maps at 0, 100, 200, 300, maximal RMS, and 500 ms. (a) task /a/, (b) task /u/, (c) control task.

Wohlert, 1993). For the control task (Fig. 3(c)), however, there is no apparent event related potential (ERP), only the background EEG activity.

Averages over 50 epochs were calculated for each task of subject S1 (Fig. 4(a)–(c)). Each trace represents one EEG channel. Scalp maps are shown at times 0, 100, 200, 300, and 500 ms and at maximal root mean square (RMS) between 300 to 500 ms. For task /a/ (Fig. 4(a)), the scalp map at 200 ms shows left hemisphere asymmetric negativity centering in the posterior region. At 300 ms, a positive shift is seen at the posterior and medial regions with a slight right hemispheric asymmetry. The SRP peak occurs at 379 ms, with symmetric positivity centering in the medial region. Task /u/ (Fig. 4(b)) shows similar posterior negativity with a slight left hemispheric asymmetry at 200 ms. A positive shift is also seen at 300 ms in the posterior and medial regions. The SRP peak is seen at 355 ms with symmetric positivity in the medial and posterior regions. Channel averages and scalp maps of the control task (Fig. 4(c)) are shown for reference. No ERP is observed for the control task. Averages for subjects S2 and S3 showed morphologies and topographic trends similar to those of S1.

3.2. Spatial patterns

Optimal spatial filters were computed from the 30 epoch training sets, and the four most important filters were used to produce feature vectors for classification. Fig. 5(a)–(c) shows the spatial patterns for subject S1 produced in one iteration of training. Each pattern is shown as a scalp map of 64 electrodes (black dots). In Fig. 5(a), electrode locations for Fz, C3, Cz and C4 of the international 10-20 system are labeled. Topographies were produced through interpolation between filter matrix elements.

For patterns discriminating /a/ and control (Fig. 5(a)), task /a/ is represented with strong, symmetrical activity in the motor cortex region, centered at Fz (CSP1) and Cz (CSP2). The control task (right column) appears mostly flat at the motor cortex. For patterns discriminating /u/ and control (Fig. 5(b)), task /u/ also shows enhanced activity in the motor cortex centered at Cz and Fz (left column). The control task again appears mostly flat. For patterns discriminating /a/ and /u/ (Fig. 5(c)), task /a/ again shows strong, symmetrical activity in the motor cortex (CSP1), but task /u/ does not. This is understandable, as the spatial filters are designed to maximize the amplitude variances between the two tasks.

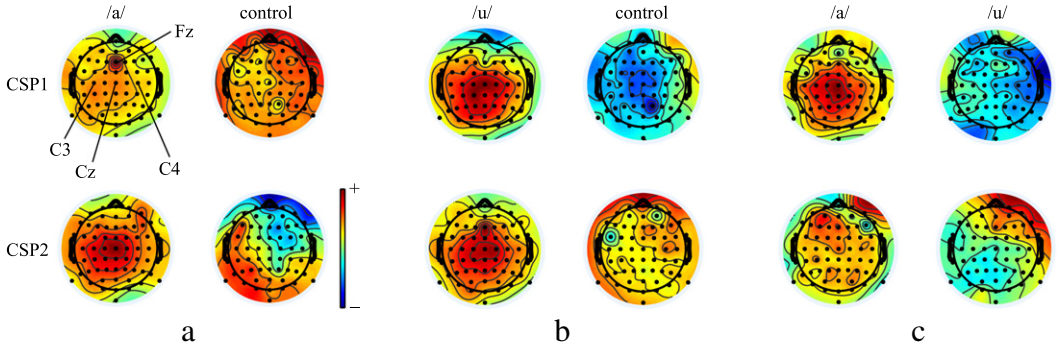

Fig. 5. The four most important common spatial patterns of each pairwise classification for subject S1. (a) /a/:control, (b) /u/:control, (c) /a/:/u/. Patterns were produced in one iteration of CSP computation using training sets of 30 epochs/task. Top row: most important patterns (CSP1), bottom row: second most important patterns (CSP2).

Table 1
Classification accuracies and standard deviations (rounded %) for 3 subjects (S1, S2 and S3) on 3 pairwise discriminations and overall. Control task is abbreviated cont. Significance threshold = 59% ($\alpha = 0.05$).

	/a/:cont.	/u/:cont.	/a/:/u/	Overall
S1	79 ± 3	82 ± 4	72 ± 3	78 ± 5
S2	71 ± 5	72 ± 4	60 ± 5	68 ± 7
S3	67 ± 4	80 ± 3	56 ± 4	68 ± 12

3.3. Classification accuracies

Table 1 shows the classification accuracies of all subjects, after 20X cross validation, for all three pairwise combinations and overall. Using χ^2 statistical analysis, significance threshold over chance was determined at 59% ($\alpha = 0.05$). Subject S1 showed the highest accuracies for all pairwise classifications and overall ($79 \pm 3, 82 \pm 4, 72 \pm 3$ and 78 ± 5 for /a/:control, /u/:control, /a/:/u/ and overall accuracy, respectively). For S2 and S3, /a/:/u/ accuracies were not significantly above chance threshold. For all subjects, pair /u/:control produced the highest accuracies, while /a/:/u/ produced the lowest.

4. Discussion

Through this study, we sought to develop a control scheme for speech prostheses using vowel speech imagery. Three major conclusions can be drawn from the results.

First, we obtained grand average waveforms for each task at electrodes in the motor cortex region. Tasks /a/ and /u/ showed SRPs similar to those seen in real speech movements (Deecke et al., 1986; Wohlert, 1993), though slightly differing in amplitude. do Nascimento, Nielsen, and Voigt (2006) showed that movement related potentials associated with imaginary plantar flexions are morphologically similar to their corresponding real movements, but also differing in amplitude. Thus, the trends are the same. Trial averages and scalp maps generated for S1 showed early left hemisphere asymmetric negativity in the posterior region. Similar topographic trends were reported as readiness potentials for imaginary plantar flexions (do Nascimento et al., 2006) and real speech movements (Deecke et al., 1986). With readiness potentials occurring in limb movement imagery and real speech movements, their occurrence in speech imagery is also to be expected.

Second, optimally discriminative spatial filters were designed for all pairwise combinations of the three tasks. When paired with the control task, both speech imagery tasks were represented with enhanced activity symmetrically located over the motor cortex region. This is expected since speech musculature is innervated from both the left and right motor cortices (Deecke et al., 1986). In addition, spatial patterns for /a/ and /u/ were similar to their respective trial-averaged scalp maps at peak RMS. This further indicates that patterns generated by the CSP method reflect SRPs. Unfortunately, although CSP has proved to be effective in EEG classification, it is not without drawbacks. Since spatial filters can only be made to distinguish between two classes, the current algorithm is limited to pairwise classifications. Also, CSP is very sensitive to noise and artifact, which can have significant effect on the spatial filters produced. This may have had some negative effect on the classification. We are currently considering multi-class alternatives shown to have improved accuracies over two-class CSP (Grosse-Wentrup & Buss, 2008). Furthermore, with the area of interest identified as the motor cortex, it may be possible, in future studies, to optimize the number of electrodes.

Third, using an SVM, we were able to perform pairwise classifications of the spatially filtered data, obtaining overall accuracies of 68%–78%. The strongest pairwise classification for all subjects was /u/:control, followed by /a/:control. These pairs alone could provide some usability for a communication BCI, such as a "yes" or "no" paradigm or a matrix selector. The reason for the lower accuracies of /a/:/u/ may have been revealed by their spatial patterns. With enhancements symmetrically located over the motor cortex region for both tasks, variance between the two tasks may be small, compared to that of the other pairs. However, despite low spatial variances between the two tasks, the algorithm can classify them with significant accuracy for S1. In addition, we are currently investigating the classification of other imaginary speech movements, such as the remaining vowels and consonants, to further broaden system usability.

It may be argued that since each task had a different visual cue, those differences could have influenced classification. However, this is unlikely to have occurred. Visual evoked potentials (VEP) are known to occur with peak latencies from 90 to 150 ms after stimulus and activations in the occipital and parietal cortices (Di Russo, Martínez, Sereno, Pitzalis, & Hillyard, 2002; Hillyard & Anllo-Vento, 1998). The phenomena observed in the current study are distinct from VEPs in both latency and topography. Furthermore, classifying neural activity elicited by such similarly presented visual stimuli may itself be a nontrivial task. A question might also be raised regarding the reproducibility of the method in a free-choice paradigm, where subjects would decide by themselves which task to perform. Although volition is certainly a component of movement related function, we believe that the SRP is a lower level process which can be produced both on cue and freely. Still, it would be useful to confirm these assumptions by implementing a single-stimulus free-choice paradigm.

A notable merit of this system is the single-trial classification, which is faster than most BCIs using averaging techniques. With the feature window being 500 ms, and task assignment by the trained classifier being nearly instantaneous, theoretical selection rate would be of the order of seconds. This would be a significant improvement over the existing communication BCIs,

with one example P300 BCI averaging 2.1 selections/min (Nijboer et al., 2008). However, the primary merit of this system is that the control scheme has a direct correlation with the desired interaction. Imagined speech movements can be conveyed as actual communication. This feature also provides benefits over existing communication BCIs. Since it is a volitive response, it does not require external stimuli like P300 BCIs. Also, the strong correlation with the desired output makes the system more natural and intuitive. This translates to improved usability and a shorter learning curve. As such, this system has significant potential as a controller for speech prostheses.

Acknowledgements

This work was supported with grants from the Japan Science and Technology Agency CREST program to Y. Sakurai and by Grants-in-Aid for Scientific Research on Priority Areas "Emergence of Adaptive Motor Function through Interaction between Body, Brain and Environment" and "Strategic Research Program for Brain Sciences" from the Ministry of Education, Culture, Sports, Science and Technology.

References

Callan, D. E., Callan, A. M., Honda, K., & Masaki, S. (2000). Single-sweep EEG analysis of neural processes underlying perception and production of vowels. *Cognitive Brain Research*, *10*, 173–176.

Chang, C., & Lin, C. (2008). *LIBSVM: A library for support vector machines (Version 2.86) [Software]*. Available from http://www.csie.ntu.edu.tw/~cjlin/libsvm.

DaSalla, C. S., Sato, M., & Koike, Y. (2007). EMG vowel recognition using a support vector machine. In I. Fragoso, F. Carnide, & F. Vieira (Eds.), *International symposium on measurement, analysis and modeling of human functions* (pp. 227–232). Lisbon: Puzzle.

Deecke, L., Engel, M., Lang, W., & Kornhuber, H. H. (1986). Bereitschaftspotential preceding speech after holding breath. *Experimental Brain Research*, *65*, 219–223.

Delorme, A., & Makeig, S. (2004). EEGLAB: An open source toolbox for analysis of single-trial EEG dynamics. *Journal of Neuroscience Methods*, *134*, 9–21.

Di Russo, F., Martínez, A., Sereno, M. I., Pitzalis, S., & Hillyard, S. A. (2002). Cortical sources of the early components of the visual evoked potential. *Human Brain Mapping*, *15*(2), 95–111.

do Nascimento, O. F., Nielsen, K. D., & Voigt, M. (2006). Movement-related parameters modulate cortical activity during imaginary isometric plantar-flexions. *Experimental Brain Research*, *171*, 78–90.

Fujimaki, N., Takeuchi, F., Kobayashi, T., Kuriki, S., & Hasuo, S. (1994). Event-related potentials in silent speech. *Brain Topography*, *6*(4), 259–267.

Gray, H. (2000). *Anatomy of the human body*. Retrieved from http://www.bartleby.com/107/.

Grosse-Wentrup, M., & Buss, M. (2008). Multiclass common spatial patterns and information theoretic feature extraction. *IEEE Transactions on Biomedical Engineering*, *55*(8), 1991–2000.

Gunn, S. R. (1998). *Support vector machines for classification and regression*. Retrieved from http://users.ecs.soton.ac.uk/srg/publications/pdf/SVM.pdf.

Hillyard, S. A., & Anllo-Vento, L. (1998). Event-related brain potentials in the study of visual selective attention. *Proceedings of the National Academy of Sciences of the United States of America*, *95*, 781–787.

Hsu, C., Chang, C., & Lin, C. (2003). *A practical guide to support vector classification*. Retrieved from http://www.csie.ntu.edu.tw/~cjlin/papers/guide/guide.pdf.

Müller-Gerking, J., Pfurtscheller, G., & Flyvbjerg, H. (1999). Designing optimal spatial filters for single-trial EEG classification in a movement task. *Clinical Neurophysiology*, *100*, 787–798.

Naito, M., Michioka, Y., Ozawa, K., Ito, Y., Kiguchi, M., & Kanazawa, T. (2007). A communication means for totally locked-in ALS patients based on changes in cerebral blood volume measured with near-infrared light. *IEICE Transactions on Information and Systems*, *E90-D*(7), 1028–1037.

Nijboer, F., Sellers, E. W., Mellinger, J., Jordan, M. A., Matuz, T., & Furdea, A. (2008). A P300-based brain–computer interface for people with amyotrophic lateral sclerosis. *Clinical Neurophysiology*, *119*(8), 1909–1916.

Oldfield, R. C. (1971). The assessment and analysis of handedness: The Edinburgh inventory. *Neuropsychologia*, *9*, 97–113.

Pfurtscheller, G., & Neuper, C. (2001). Motor imagery and direct brain-computer communication. *Proceedings of the IEEE*, *87*(7), 1123–1134.

Ramoser, H., Müller-Gerking, J., & Pfurtscheller, G. (2000). Optimal spatial filtering of single trial EEG during imagined hand movement. *IEEE Transactions on Rehabilitation Engineering*, *8*(4), 441–446.

Wohlert, A. (1993). Event-related brain potentials preceding speech and nonspeech oral movements of varying complexity. *Journal of Speech and Hearing Research*, *36*, 897–905.